PERGAMON

International Journal of Solids and Structures 40 (2003) 5781–5797

INTERNATIONAL JOURNAL OF SOLIDS and STRUCTURES

www.elsevier.com/locate/ijsolstr

Edge dislocation interacting with an interfacial crack along a circular inhomogeneity

Q.H. Fang [a], Y.W. Liu [a,*], C.P. Jiang [b]

[a] *Department of Engineering Mechanics, Hunan University, Changsha 410082, PR China*

[b] *Solid Mechanics Research Center, Beijing University of Aeronautics and Astronautics, Beijing 100083, PR China*

Received 24 December 2002; received in revised form 2 June 2003

Abstract

The elastic interaction of an edge dislocation, which is located either outside or inside a circular inhomogeneity, with an interfacial crack is dealt with. Using Riemann–Schwarz's symmetry principle integrated with the analysis of singularity of the complex potentials, the closed form solutions for the elastic fields in the matrix and inhomogeneity regions are derived explicitly. The image force on the dislocation is then determined by using the Peach–Keohler formula. The influence of the crack geometry and material mismatch on the dislocation force is evaluated and discussed when the dislocation is located in the matrix. It is shown that the interfacial crack has significant effect on the equilibrium position of the edge dislocation near a circular interface. The results also reveal a strong dependency of the dislocation force on the mismatch of the shear moduli and Poisson's ratios between the matrix and inhomogeneity.

Keywords: Edge dislocation; Circular interfacial crack; Dislocation force; Complex variable method

1. Introduction

The elastic interaction between a dislocation and inhomogeneities is very important in studying the mechanical behavior of many materials. The study of a dislocation interacting with an inhomogeneity in the solid mechanics and materials science is motivated by the need for a better understanding of the mechanism of strengthening and toughening of materials. A comprehensive survey of the theoretical investigation on this topic has been provided by Dundurs (1969).

Due to its importance, this problem has received much attention during the last several decades. The first investigation to assess the interaction of a screw dislocation with an inhomogeneity was performed by Head (1953), who considered a dislocation near an interface between two dissimilar materials. The force on the dislocation was analyzed and a simple attraction–repulsion criterion was given in the paper. For the

* Corresponding author. Tel.: +86-731-8821889; fax: +86-731-8822330.
E-mail address: liuyouw8294@sina.com (Y.W. Liu).

0020-7683/$ - see front matter © 2003 Published by Elsevier Ltd.
doi:10.1016/S0020-7683(03)00338-X

interaction problem of an edge dislocation near a circular inclusion in fiber-reinforced composites, Dundurs and Mura (1964) and Dundurs and Sendeckyj (1965) indicated that under certain conditions the dislocation may even have a stable equilibrium position at a distance from the circular inclusion interface. Smith (1968) considered the interaction between a screw dislocation and a circular elastic inhomogeneity, and extended the theory to treat the case of a dislocation interacting with an elliptic hole or a rigid elliptic inhomogeneity under longitudinal shear. He calculated the interactive stress field on the x-axis. The interaction between a screw dislocation and an elliptic elastic inhomogeneity had been studied by Gong and Meguid (1994). The appropriate expressions of the interacting energy and the force on dislocation were explicitly derived in that article. Luo and Chen (1991) evaluated the interaction energy and the force acting on an edge dislocation when dislocation was located inside the interphase layer based on a three phase composite cylinder model. Qaissaunee and Santare (1995) investigated the interaction effect of an edge dislocation, which is located inside the inhomogeneity or inside the matrix, with an elliptic inclusion based on a three phase elliptic cylinder model. Xiao and Chen (2000, 2001) considered a screw dislocation and an edge dislocation interacting with a coated circular inclusion, respectively. The force acting on the dislocation was calculated and the equilibrium positions of the dislocation were discussed for various material property combinations and variations in coating thickness. In addition, Lung and Wang (1984) and Lee (1987) evaluated the image force on a screw dislocation near a finite length crack tip and analyzed the influence of the crack length on the image force.

Interfacial defects, typically interfacial cracks, are produced inevitably in manufacturing and using of composite materials. Therefore, the investigation on the interaction between a dislocation and an inhomogeneity with interfacial defects is of practical importance. Such an investigation can improve the understanding of strengthening and hardening mechanism of materials and offer a scientific basis for the establishment of the interface fracture criterion between dissimilar materials.

The problem of an edge dislocation interacting with a circular interfacial crack is studied in the present work, where the dislocation is located inside the inhomogeneity or inside the matrix. Using Riemann–Schwarz's symmetry principle integrated with the analysis of singularity of complex functions (Toya, 1974; Liu, 1991), we obtain the closed form solutions. The explicit expressions of the stress functions and the image dislocation force are derived and the influence of the crack on the force acting on the dislocation is discussed and shown graphically. When the length of the crack goes to zero, the present solutions degenerate into ones for the problem of a circular elastic inhomogeneity with a perfect bonding interface (Dundurs and Mura, 1964; Dundurs and Sendeckyj, 1965).

2. Problem statement and basic formulation

The physical problem to be considered is shown in Fig. 1. Let an infinite matrix S^- with the elastic properties κ_2 and μ_2 contain a partially bonded circular inclusion S^+ of a radius R with the elastic properties κ_1 and μ_1, where $\mu_j (j = 1, 2)$ is the shear modulus and $\kappa_j = 3 - 4\upsilon_j$ for plane strain or $\kappa_j = (3 - 4\upsilon_j)/(1 + \upsilon_j)$ for generalized plane stress conditions, υ_j is the Poisson's ratio, respectively. It is assumed that an interfacial crack lies along an arc L with the end points a and b $(a = \mathrm{Re}^{\mathrm{i}\alpha_1}, b = \mathrm{Re}^{\mathrm{i}\alpha_2})$ in the interface while along the remaining part of the interface, L', the inclusion is well bonded to the matrix. An edge dislocation with Burger's vector (b_x, b_y) is located at an arbitrary point in the matrix or inside inhomogeneity.

Let the center of the circular inhomogeneity be at the origin of the complex plane $z = x + \mathrm{i}y$ and $t = \mathrm{Re}^{\mathrm{i}\theta}$ be the points of on the interface. The boundary conditions of the displacement and stress for the present problem can be expressed as follows:

$$u_1^+(t) + \mathrm{i}v_1^+(t) = u_2^-(t) + \mathrm{i}v_2^-(t) \quad t \in L' \tag{1}$$

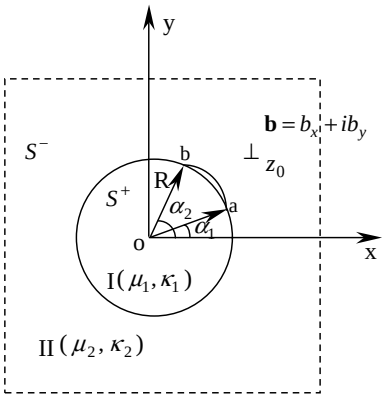

Fig. 1. An edge dislocation interacting with a circular interfacial crack.

$$\sigma^+_{rr1}(t) + \mathrm{i}\tau^+_{r\theta 1}(t) = \sigma^-_{rr2}(t) + \mathrm{i}\tau^-_{r\theta 2}(t) \quad t \in L' \tag{2}$$

and

$$\sigma^+_{rr1}(t) + \mathrm{i}\tau^+_{r\theta 1}(t) = 0 \quad t \in L \tag{3}$$

$$\sigma^-_{rr2}(t) + \mathrm{i}\tau^-_{r\theta 2}(t) = 0 \quad t \in L \tag{4}$$

where σ_{rr} and $\tau_{r\theta}$ are the components of the stress in polar coordinates, u and v are the components of the displacement in the Cartesian coordinates, the subscripts 1 and 2 represent the regions S^+ and S^-, the superscripts + and − denote the boundary values of the physical quantity as z approaches to the interface from S^+ and S^-, respectively.

The elastic field in the medium may be expressed in term of Muskhelishvili's complex potentials $\Phi(z)$ and $\Psi(z)$. In the polar coordinates the stress and displacement fields may be expressed as:

$$\sigma_{rr} + \sigma_{\theta\theta} = 2[\Phi(z) + \overline{\Phi(z)}] \tag{5}$$

$$\sigma_{rr} + \mathrm{i}\tau_{r\theta} = \Phi(z) + \overline{\Phi(z)} - \bar{z}\overline{\Phi'(z)} - \bar{z}/z\overline{\Psi(z)} \tag{6}$$

$$2\mu(u' + v') = \mathrm{i}z\left[\kappa\Phi(z) - \overline{\Phi(z)} + \bar{z}\overline{\Phi'(z)} + \frac{\bar{z}}{z}\overline{\Psi(z)}\right] \tag{7}$$

where $u' = \partial u/\partial\theta$, $v' = \partial v/\partial\theta$, $\Phi'(z) = \mathrm{d}[\Phi(z)]/\mathrm{d}z$, the over-bar represents the complex conjugate.

3. Analysis and solutions

3.1. Edge dislocation in the matrix

Consider the problem of an edge dislocation with Burger's vector (b_x, b_y) located at an arbitrary point z_0 inside the region S^- (matrix). In the matrix, we define the complex potentials as:

$$\Phi_2(z) = \Phi^*_2(z) + \Phi_0(z) \quad z \in S^- \tag{8}$$

$$\Psi_2(z) = \Psi^*_2(z) + \Psi_0(z) \quad z \in S^- \tag{9}$$

where $\Phi_0(z)$ and $\Psi_0(z)$ represent the complex potentials for an edge dislocation in an infinite homogeneous matrix in the absence of the inhomogeneity and $\Phi_2^*(z)$ and $\Psi_2^*(z)$ refer to the terms of the disturbance of the complex potentials due to the presence of the inhomogeneity and the interfacial crack.

The complex potentials for an edge dislocation at the point z_0 in a homogeneous matrix can be expressed as:

$$\Phi_0(z) = \frac{\gamma_2}{z - z_0} \tag{10}$$

$$\Psi_0(z) = \frac{\overline{\gamma_2}}{z - z_0} + \frac{\gamma_2 \bar{z}_0}{(z - z_0)^2} \tag{11}$$

where $\gamma_2 = \frac{\mu_2}{\pi(1+\kappa_2)}(b_y - \mathrm{i}b_x)$.

Applying Riemann–Schwarz's symmetry principle, we extend the definition of the analytical function $\Phi_2(z)$ into the region S^+ across L by introducing (Toya, 1974)

$$\Phi_2\left(\frac{R^2}{\bar{z}}\right) = -\overline{\Phi_2(z)} + \bar{z}\overline{\Phi_2'(z)} + \frac{\bar{z}^2}{R^2}\overline{\Psi_2(z)} \tag{12}$$

or equivalently, writing R^2/z for $\bar{z}$,

$$\Phi_2(z) = -\overline{\Phi_2}\left(\frac{R^2}{z}\right) + \frac{R^2}{z}\overline{\Phi_2'}\left(\frac{R^2}{z}\right) + \frac{R^2}{z^2}\overline{\Psi_2}\left(\frac{R^2}{z}\right) \tag{13}$$

where $\Phi_2(z)$ is holomorphic everywhere in the region S^+ except at the points $z = R^2/\bar{z}_0$ and $z = 0$ where it is singular. The substitution of Eqs. (8) and (9) into Eq. (13) yields

$$\Phi_2(z) = G(z) + \Phi_{20}(z) \tag{14}$$

where

$$G(z) = \frac{\gamma_2}{z - z_0} + \frac{\gamma_2}{z} - \frac{\gamma_2}{z - z^*} + \frac{\overline{\gamma_2} z^*(z_0 - z^*)}{\bar{z}_0(z - z^*)^2}, \quad z^* = \frac{R^2}{\bar{z}_0}$$

Functions $\Phi_1(z)$ and $\Psi_1(z)$ are holomorphic in the region S^+ because there is no point force or dislocation in the inclusion. Similarly, extend the function $\Phi_1(z)$ from S^+ to S^- by introducing:

$$\Phi_1(z) = -\overline{\Phi_1}\left(\frac{R^2}{z}\right) + \frac{R^2}{z}\overline{\Phi_1'}\left(\frac{R^2}{z}\right) + \frac{R^2}{z^2}\overline{\Psi_1}\left(\frac{R^2}{z}\right) \tag{15}$$

where $\Phi_1(z)$ is holomorphic on the entire plane cut along L' except at the point at infinity.

Taking the complex conjugate of Eqs. (13) and (15), It is found that

$$\Psi_1(z) = \frac{R^2}{z^2}\left[\Phi_1(z) + \overline{\Phi_1}\left(\frac{R^2}{z}\right) - z\Phi_1'(z)\right] \tag{16}$$

$$\Psi_2(z) = \frac{R^2}{z^2}\left[\Phi_2(z) + \overline{\Phi_2}\left(\frac{R^2}{z}\right) - z\Phi_2'(z)\right] \tag{17}$$

Substituting Eq. (6) into Eq. (2), and considering Eqs. (3) and (4), the traction continuity condition on the entire circular boundary can be written as:

$$[\Phi_1(t) + \Phi_2(t)]^+ = [\Phi_1(t) + \Phi_2(t)]^- \quad t \in L + L' \tag{18}$$

It is seen that the function $\Xi(z) = \Phi_1(z) + \Phi_2(z)$ is holomorphic in the entire plane except at points $z = z_0$, $z = R^2/\bar{z}_0$ and $z = 0$. According to the generalized Liouville's theorem, Eq. (18) leads to

$$\Xi(z) = G(z) + D_0 \tag{19}$$

Comparing Eqs. (14) and (19), we obtain

$$D_0 = -\overline{\Phi_1(0)} \tag{20}$$

Taking the derivatives with respect to θ of Eq. (1), then substituting Eq. (7) into Eq. (1), the displacement boundary condition can be expressed as:

$$\frac{\kappa_1}{2\mu_1}\Phi_1^+(t) + \frac{1}{2\mu_1}\Phi_1^-(t) = \frac{\kappa_2}{2\mu_2}\Phi_2^-(t) + \frac{1}{2\mu_2}\Phi_2^+(t) \tag{21}$$

Substituting Eq. (19) into Eq. (21), and noting Eqs. (8) and (9), the above equation can be written as follows:

$$\Phi_{20}^+(t) - g\Phi_{20}^-(z) = hG(t) + KD_0 \quad t \in L' \tag{22}$$

where

$$g = -\frac{\mu_2 + \kappa_2\mu_1}{\mu_1 + \kappa_1\mu_2}, \quad h = -\frac{\mu_1(1+\kappa_2)}{\mu_1 + \kappa_1\mu_2}, \quad K = \frac{\mu_2(1+\kappa_1)}{\mu_1 + \kappa_1\mu_2}$$

Referring to Muskhelishvili (1975), the general solution is given formally by

$$\Phi_{20}(z) = \frac{X_0(z)}{2\pi\mathrm{i}}\int_b^a \frac{hG(t) + KD_0}{X_0^+(t)}\frac{\mathrm{d}t}{t-z} + X_0(z)(C_0 + C_1 z) \tag{23}$$

where $X_0(z) = (z-a)^{-\frac{1}{2}-\mathrm{i}\beta}\cdot(z-b)^{-\frac{1}{2}+\mathrm{i}\beta}$, $\beta = \frac{\ln|g|}{2\pi}$.

The Plemelj function $X_0(z)$ is a single-valued branch in the plane cut along L'. The function satisfies the relation $X_0^+(t) = gX_0^-(t)$ on L, and for which

$$\lim_{|z|\to\infty} zX_0(z) = 1 \tag{24}$$

The holomorphic function $\Phi_{20}(z)$ vanishes at infinity. Comparing the expansions of Eqs. (8) and (23) at infinity, and noting Eq. (24), the unknown constant C_1 can be determined.

$$C_1 = 0 \tag{25}$$

The complex potential $\Phi_2(z)$ is holomorphic and takes the following form for a large value of $|z|$

$$\Phi_2(z) = \frac{\gamma_2}{z} + o\left(\frac{1}{z^2}\right) \tag{26}$$

After evaluating the Cauchy integral in Eq. (23), we obtain

$$\Phi_{20}(z) = \frac{hG(z) + KD_0}{1-g} - \frac{X_0(z)}{1-g}[G_0(z) + G_\infty(z) + G_{z_0}(z) + G_{z^*}(z) - (1-g)C_0] \tag{27}$$

where $G_0(z) = \frac{h\gamma_2}{z}\frac{1}{X_0(0)}$

$$G_\infty(z) = \left[z - \frac{R}{2}(\exp[\mathrm{i}\alpha_1] + \exp[\mathrm{i}\alpha_2]) - \mathrm{i}R\beta(\exp[\mathrm{i}\alpha_1] - \exp[\mathrm{i}\alpha_2])\right]KD_0 + h\gamma_2$$

$$G_{z_0}(z) = \frac{h\gamma_2}{X_0(z_0)}\frac{1}{z - z_0}$$

$$G_{z^*}(z)=\frac{h}{X_0(z^*)}\left\{\frac{z^*(z_0-z^*)\overline{\gamma_2}}{\overline{z_0}(z-z^*)^2}\left[1-(z-z^*)\frac{X_0'(z^*)}{X_0(z^*)}\right]-\frac{\gamma_2}{z-z^*}\right\}$$

Substituting Eq. (27) into Eq. (14), $\Phi_2(z)$ can be evaluated:

$$\Phi_2(z)=\frac{K}{1-g}[G(z)+D_0]-\frac{X_0(z)}{1-g}\left[G_0(z)+G_\infty(z)+G_{z_0}(z)+G_{z^*}(z)-(1-g)C_0\right] \tag{28}$$

The substitution of Eq. (28) into Eq. (19) yields:

$$\Phi_1(z)=-\frac{h}{1-g}[G(z)+D_0]+\frac{X_0(z)}{1-g}[G_0(z)+G_\infty(z)+G_{z_0}(z)+G_{z^*}(z)-(1-g)C_0] \tag{29}$$

Expanding $\Phi_2(z)$ at $|z|=\infty$ and comparing with Eq. (26), the unknown constant C_0 can be determined.

$$C_0=0 \tag{30}$$

Substituting Eq. (29) into Eq. (20), and noting

$$\frac{X_0(z)}{1-g}\frac{1}{X_0(0)}\frac{h\gamma_2}{z}-\frac{1}{1-g}\frac{\gamma_2}{z}=\frac{h\gamma_2}{1-g}\frac{X_0'(0)}{X_0(0)} \tag{31}$$

at $z=0$, we obtain

$$D_0=\frac{QQ_1-\overline{Q_1}}{1-Q^2} \tag{32}$$

where

$$Q=\frac{-K}{1-g}X_0(0)R\left[\frac{1}{2}(\exp[\mathrm{i}\alpha_1]+\exp[\mathrm{i}\alpha_2])+\mathrm{i}\beta(\exp[\mathrm{i}\alpha_1]-\exp[\mathrm{i}\alpha_2])\right]-\frac{K}{1-g}+1$$

$$Q_1=\frac{h\gamma_2}{1-g}\frac{X_0'(0)}{X_0(0)}+\frac{hX_0(0)}{1-g}\left\{\frac{\overline{\gamma_2}(z_0-z^*)}{\overline{z}_0X_0(z^*)}\left[\frac{\bar{z}_0}{R^2}+\frac{X_0'(z^*)}{X_0(z^*)}\right]+\gamma_2-\frac{\gamma_2}{z_0X_0(z_0)}+\frac{\gamma_2}{z^*X_0(z^*)}\right\}$$
$$-\frac{h}{1-g}\left[\frac{\gamma_2}{z^*}+\frac{\overline{\gamma_2}(z_0-z^*)}{\overline{z_0}z^*}-\frac{\gamma_2}{z_0}\right]$$

Once the stress functions $\Phi_1(z)$ and $\Phi_2(z)$ are known, the stress functions $\Psi_1(z)$ and $\Psi_2(z)$ may be determined by Eqs. (16) and (17), respectively. The components of the stress and displacement may also be determined from Eqs. (5)–(7).

3.2. Edge dislocation inside the inhomogeneity

An edge dislocation with Burger's vector (b_x,b_y) is located at an arbitrary point z_0 inside the region S^+ (inhomogeneity). In the same manner as in Section 3.1, we define the potentials in the inhomogeneity as follows:

$$\Phi_1(z)=\Phi_1^*(z)+\Phi_0(z)\quad z\in S^+ \tag{33}$$

$$\Psi_1(z)=\Psi_1^*(z)+\Psi_0(z)\quad z\in S^+ \tag{34}$$

where $\Phi_1^*(z)$ and $\Psi_1^*(z)$ will be determined later, and

$$\Phi_0(z)=\frac{\gamma_1}{z-z_0} \tag{35}$$

$$\Psi_0(z) = \frac{\overline{\gamma_1}}{z - z_0} + \frac{\gamma_1 \bar{z}_0}{(z - z_0)^2} \tag{36}$$

where $\gamma_1 = \frac{\mu_1}{\pi(1+\kappa_1)}(b_y - \mathrm{i}b_x)$.

The complex potentials outside the inhomogeneity are holomorphic and take the following forms for a large value of $|z|$.

$$\Phi_2(z) = \frac{\gamma_2}{z} + o\left(\frac{1}{z^2}\right), \quad \Psi_2(z) = \frac{\overline{\gamma_2}}{z} + o\left(\frac{1}{z^2}\right) \tag{37}$$

Using the same method as in Section 3.1, the complex potentials inside the inhomogeneity and matrix can be expressed as follows:

$$\Phi_1(z) = -\frac{h}{1-g}\left[G^*(z) + D_0^* + \frac{\gamma_2}{z}\right] + \frac{X_0(z)}{1-g}\left[G_0^*(z) + G_\infty^*(z) + G_{z_0}^*(z) + G_{z^*}^*(z)\right] \tag{38}$$

$$\Phi_2(z) = \frac{K}{1-g}\left[G^*(z) + D_0^* + \frac{\gamma_2}{z}\right] - \frac{X_0(z)}{1-g}\left[G_0^*(z) + G_\infty^*(z) + G_{z_0}^*(z) + G_{z^*}^*(z)\right] \tag{39}$$

where

$$G^*(z) = \frac{\gamma_1}{z - z_0} - \frac{\gamma_1}{z - z^*} + \frac{\overline{\gamma_2} z^*(z_0 - z^*)}{\bar{z}_0(z - z^*)^2} \quad z^* = \frac{R^2}{\overline{z_0}}$$

$$G_0^*(z) = \frac{h\gamma_2}{z}\frac{1}{X_0(0)}$$

$$G_\infty^*(z) = \left[z - \frac{R}{2}(\exp[\mathrm{i}\alpha_1] + \exp[\mathrm{i}\alpha_2]) - \mathrm{i}R\beta(\exp[\mathrm{i}\alpha_1] - \exp[\mathrm{i}\alpha_2])\right]KD_0^* + h\gamma_2$$

$$G_{z_0}^*(z) = \frac{K\gamma_1}{X_0(z_0)}\frac{1}{z - z_0}$$

$$G_{z^*}^*(z) = \frac{K}{X_0(z^*)}\left\{\frac{z^*(z_0 - z^*)\overline{\gamma_1}}{\bar{z}_0(z - z^*)^2}\left[1 - (z - z^*)\frac{X_0'(z^*)}{X_0(z^*)}\right] - \frac{\gamma_1}{z - z^*}\right\}$$

$$D_0^* = \frac{Q^* Q_1^* - \overline{Q_1^*}}{1 - Q^* \ * \ Q^*}$$

$$Q^* = \frac{-K}{1-g}X_0(0)R\left[\frac{1}{2}(\exp[\mathrm{i}\alpha_1] + \exp[\mathrm{i}\alpha_2]) + \mathrm{i}\beta(\exp[\mathrm{i}\alpha_1] - \exp[\mathrm{i}\alpha_2])\right] - \frac{K}{1-g} + 1$$

$$Q_1^* = \frac{h\gamma_2}{1-g}\frac{X_0'(0)}{X_0(0)} + \frac{X_0(0)}{1-g}\left\{\frac{K\overline{\gamma_1}(z_0 - z^*)}{\overline{z_0}X_0(z^*)}\left[\frac{\overline{z_0}}{R^2} + \frac{X_0'(z^*)}{X_0(z^*)}\right] + h\gamma_2 - \frac{K\gamma_1}{z_0 X_0(z_0)} + \frac{K\gamma_1}{z^* X_0(z^*)}\right\}$$
$$- \frac{h}{1-g}\left[\frac{\gamma_1}{z^*} + \frac{\overline{\gamma_1}(z_0 - z^*)}{\overline{z_0}z^*} - \frac{\gamma_1}{z_0}\right]$$

The stress functions $\Psi_1(z)$ and $\Psi_2(z)$ may be determined from Eqs. (16) and (17), respectively. The components of the stress and displacement may also be determined from Eqs. (5)–(7).

4. Perturbation stress functions and image force on the dislocation

4.1. Edge dislocation in the matrix

For the dislocation-inclusion-interfacial crack interaction problems, a common measure of the stress field is the Peach–Keohler force (Hirth and Lothe, 1982), which is a measure of the force on dislocation due to its interaction with the inclusion and interfacial crack. This force on the dislocation arises from both the presence of the dislocation and the fact that there exist a material mismatch and an interfacial crack. If there is no material mismatch and no crack, the force on the dislocation is zero. The image force on the dislocation is a significant physical quantity for understanding the interacting mechanism of a dislocation and an inhomogeneity. The image force can be obtained by the Peach–Keohler formula as:

$$F_x - \mathrm{i}F_y = \left[\widehat{\tau}_{xy}(z_0)b_x + \widehat{\sigma}_{yy}(z_0)b_y\right] + \mathrm{i}\left[\widehat{\sigma}_x(z_0)b_{xx} + \widehat{\tau}_{xy}(z_0)b_y\right] \tag{40}$$

where $\widehat{\sigma}_x, \widehat{\sigma}_y, \widehat{\tau}_{xy}$ are the components of the perturbation stress at the dislocation in the Cartesian coordinates.

Referring to Muskhelishvili (1975), the stress fields are related to the complex potentials through

$$\begin{aligned}
\sigma_{xx} &= \mathrm{Re}[2\Phi(z) - \bar{z}\Phi'(z) - \Psi(z)] \\
\sigma_{yy} &= \mathrm{Re}[2\Phi(z) + \bar{z}\Phi'(z) + \Psi(z)] \\
\tau_{xy} &= \mathrm{Im}[\bar{z}\Phi'(z) + \Psi(z)]
\end{aligned} \tag{41}$$

When the edge dislocation is located at the point z_0 in the matrix, the perturbation stresses can be evaluated by the perturbation stress functions, $\Phi_2^*(z_0)$, $\Phi_2^{*\prime}(z_0)$ and $\Psi_2^*(z_0)$ in the matrix. In terms of Eq. (41) the Peach–Keohler force can be written as

$$F_x - \mathrm{i}F_y = \frac{\mu_2(b_y^2 + b_x^2)}{\pi(1+\kappa_2)}\left[\frac{\Phi_2^*(z_0) + \overline{\Phi_2^*(z_0)}}{\gamma_2} + \frac{\bar{z}_0\Phi_2^{*\prime}(z_0) + \Psi_2^*(z_0)}{\overline{\gamma_2}}\right] \tag{42}$$

According to Qaissaunee and Santare (1995) and from Eqs. (8) and (9), the functions $\Phi_2^*(z_0)$, $\Phi_2^{*\prime}(z_0)$ and $\Psi_2^*(z_0)$ may be determined as follows:

$$\Phi_2^*(z_0) = \lim_{z\to z_0}[\Phi_2(z) - \Phi_0(z)] \tag{43}$$

$$\Phi_2^{*\prime}(z_0) = \lim_{z\to z_0}\frac{\mathrm{d}[\Phi_2(z) - \Phi_0(z)]}{\mathrm{d}z} \tag{44}$$

$$\Psi_2^*(z_0) = \lim_{z\to z_0}[\Psi_2(z) - \Psi_0(z)] \tag{45}$$

Substituting Eqs. (30) and (32) into Eq. (28), we obtain

$$\begin{aligned}
\Phi_2(z) = {} & \frac{h+1-g}{1-g}\left[\frac{\gamma_2}{z} + \frac{\gamma_2}{z-z_0} - \frac{\gamma_2}{z-z^*} + \frac{\overline{\gamma_2}z^*(z_0-z^*)}{\overline{z_0}(z-z^*)^2}\right] + \frac{KD_0}{1-g} - \frac{X_0(z)}{1-g}\left\{\frac{h\gamma_2 R}{z}\exp\left[\frac{\mathrm{i}}{2}(\alpha_1+\alpha_2)\right.\right. \\
& \left.\left. + \beta(\alpha_2-\alpha_1-2\pi)\right] + KD_0 z + h\gamma_2 - \frac{R}{2}(\exp[\mathrm{i}\alpha_1] + \exp[\mathrm{i}\alpha_2]) - \mathrm{i}R\beta(\exp[\mathrm{i}\alpha_1] - \exp[\mathrm{i}\alpha_2])KD_0\right. \\
& \left. + \frac{h\gamma_2}{X_0(z_0)}\frac{1}{z-z_0} + \frac{h\overline{\gamma_2}}{X_0(z^*)}\frac{z^*(z_0-z^*)}{\bar{z}_0(z-z^*)^2}\left[1 - (z-z^*)\frac{X_0'(z^*)}{X_0(z^*)}\right] - \frac{h\gamma_2}{X_0(z^*)}\frac{1}{z-z^*}\right\}
\end{aligned} \tag{46}$$

Substituting Eq. (28) into (17), we obtain

$$\begin{aligned}\Psi_2(z)=\frac{R^2}{z^2}\Bigg\{&\frac{h+1-g}{1-g}\left[\frac{2\gamma_2}{z}+\frac{\gamma_2}{z-z_0}-\frac{\gamma_2}{z-z^*}+\frac{\overline{\gamma_2}z^*(z_0-z^*)}{\overline{z_0}(z-z^*)}+\frac{\overline{\gamma_2}z}{R^2}+\frac{\overline{\gamma_2}z}{R^2-\overline{z_0}z}-\frac{\overline{\gamma_2}z_0z}{R^2(z_0-z)}\right.\\&\left.+\frac{\gamma_2(z_0\overline{z_0}-R^2)z^2}{R^2z_0(z-z_0)^2}+\frac{\gamma_2z}{(z-z_0)^2}+\frac{2\overline{\gamma_2}z^*(z_0-z^*)z}{\overline{z_0}(z-z^*)^3}-\frac{\gamma_2z}{(z-z^*)^2}\right]+\frac{K(D_0+\overline{D_0})}{1-g}\\&-\frac{X_0(z)}{1-g}\left[\frac{2h\gamma_2R}{z}\exp\left[\frac{\mathrm{i}}{2}(\alpha_1+\alpha_2)+\beta(\alpha_2-\alpha_1-2\pi)\right]+KD_0z+h\gamma_2-(R-z)\left(\frac{1}{2}\exp[\mathrm{i}\alpha_1]\right.\right.\\&\left.+\frac{1}{2}\exp[\mathrm{i}\alpha_2]+\mathrm{i}\beta\exp[\mathrm{i}\alpha_1]-\mathrm{i}\beta\exp[\mathrm{i}\alpha_2]\right)+\frac{h\gamma_2}{X_0(z_0)}\frac{1}{z-z_0}+\frac{h\gamma_2}{X_0(z_0)}\frac{z}{(z-z_0)^2}\\&+\frac{h\overline{\gamma_2}}{X_0(z^*)}\frac{z^*(z_0-z^*)}{\overline{z_0}(z-z^*)^2}-\frac{h\overline{\gamma_2}}{X_0(z^*)}\frac{z^*(z_0-z^*)}{\overline{z_0}(z-z^*)}\frac{X_0'(z^*)}{X_0(z^*)}+\frac{2h\overline{\gamma_2}}{X_0(z^*)}\frac{z^*(z_0-z^*)z}{\overline{z_0}(z-z^*)^3}\\&\left.-\frac{h\overline{\gamma_2}}{X_0(z^*)}\frac{z^*(z_0-z^*)z}{\overline{z_0}(z-z^*)^2}\frac{X_0'(z^*)}{X_0(z^*)}-\frac{h\gamma_2}{X_0(z^*)}\frac{z}{(z-z^*)^2}-\frac{h\gamma_2}{X_0(z^*)}\frac{1}{z-z^*}\right]\\&-\frac{X_0(z_1)}{1-g}\left[\frac{h\overline{\gamma_2}R}{z_1}\exp\left[\frac{-\mathrm{i}}{2}(\alpha_1+\alpha_2)+\beta(\alpha_2-\alpha_1-2\pi)\right]+K\overline{D_0}z_1+h\overline{\gamma_2}\right.\\&-R\left(\frac{1}{2}\exp[-\mathrm{i}\alpha_1]+\frac{1}{2}\exp[-\mathrm{i}\alpha_2]-\mathrm{i}\beta\exp[-\mathrm{i}\alpha_1]+\mathrm{i}\beta\exp[-\mathrm{i}\alpha_2]\right)K\overline{D_0}+\frac{h\overline{\gamma_2}}{\overline{X_0(z_0)}}\frac{1}{z_1-\overline{z_0}}\\&+\frac{h\gamma_2}{X_0(z^*)}\frac{\overline{z^*}(\overline{z_0}-\overline{z^*})}{z_0(z_1-\overline{z^*})^2}-\frac{h\gamma_2}{\overline{X_0(z^*)}}\frac{\overline{z^*}(\overline{z_0}-\overline{z^*})}{z_0(z_1-\overline{z^*})}\frac{\overline{X_0'(z^*)}}{\overline{X_0(z^*)}}-\frac{h\overline{\gamma_2}}{\overline{X_0(z^*)}}\frac{1}{z_1-\overline{z^*}}\Bigg]\\&+\frac{X_0'(z)z}{1-g}\left[\frac{h\gamma_2R}{z}\exp\left[\frac{\mathrm{i}}{2}(\alpha_1+\alpha_2)+\beta(\alpha_2-\alpha_1-2\pi)\right]+KD_0z+h\gamma_2\right.\\&-R\left(\frac{1}{2}\exp[\mathrm{i}\alpha_1]+\frac{1}{2}\exp[\mathrm{i}\alpha_2]+\mathrm{i}\beta\exp[\mathrm{i}\alpha_1]-\mathrm{i}\beta\exp[\mathrm{i}\alpha_2]\right)KD_0+\frac{h\gamma_2}{X_0(z_0)}\frac{1}{z-z_0}\\&\left.+\frac{h\overline{\gamma_2}}{X_0(z^*)}\frac{z^*(z_0-z^*)}{\overline{z_0}(z-z^*)^2}-\frac{h\overline{\gamma_2}}{X_0(z^*)}\frac{z^*(z_0-z^*)}{\overline{z_0}(z-z^*)}\frac{X_0'(z^*)}{X_0(z^*)}-\frac{h\gamma_2}{X_0(z^*)}\frac{1}{z-z^*}\right]\Bigg\}\end{aligned}\tag{47}$$

where

$$\frac{X_0'(z^*)}{X_0(z^*)}=-\frac{z^*-(a+b)+2\mathrm{i}(a-b)}{2(z^*-a)(z^*-b)},\quad z_1=\frac{R^2}{z}$$

Letting $\alpha=0$ and noting

$$X_0(z)=\frac{g}{z-R}\quad z\in S^+\tag{48}$$

$$X_0(z)=\frac{1}{z-R}\quad z\in S^-\tag{49}$$

Eqs. (46) and (47) are reduced to the solutions of the interaction problem between an edge dislocation and a circular inhomogeneity, which are in agreement with the reduced results of Xiao and Chen (2000). Here we omit details for saving space.

Substituting Eqs. (46) and (47) into Eqs. (43)–(45), the perturbation stress functions can be expressed as:

$$\begin{aligned}\Phi_2^*(z_0) = {} & \frac{K}{1-g}\left[\frac{\gamma_2}{z_0} - \frac{\gamma_2}{z_0 - z^*} + \frac{\overline{\gamma_2} z^*}{\overline{z_0}(z_0 - z^*)} + D_0\right] - \frac{X_0(z_0)}{1-g}\left[\frac{h\gamma_2 R}{z_0}\exp\left[\frac{\mathrm{i}}{2}(\alpha_1+\alpha_2) + \beta(\alpha_2 - \alpha_1 - 2\pi)\right]\right. \\ & + KD_0 z_0 + h\gamma_2 - R\left(\frac{1}{2}\exp[\mathrm{i}\alpha_1] + \frac{1}{2}\exp[\mathrm{i}\alpha_2] + \mathrm{i}\beta\exp[\mathrm{i}\alpha_1] - \mathrm{i}\beta\exp[\mathrm{i}\alpha_2]\right)KD_0 \\ & \left. + \frac{h\overline{\gamma_2}}{X_0(z^*)}\frac{z^*}{\overline{z_0}(z_0 - z^*)} - \frac{h\overline{\gamma_2}}{X_0(z^*)}\frac{z^*}{\overline{z_0}}\frac{X_0'(z^*)}{X_0(z^*)} - \frac{h\gamma_2}{X_0(z^*)}\frac{1}{z_0 - z^*}\right] - \frac{h\gamma_2}{1-g}\frac{X_0'(z_0)}{X_0(z_0)}\end{aligned} \tag{50}$$

$$\begin{aligned}\Phi_2^{*\prime}(z_0) = {} & \frac{K}{1-g}\left[-\frac{\gamma_2}{z_0^2} + \frac{\gamma_2}{(z_0 - z^*)^2} - \frac{2\overline{\gamma_2} z^*}{\overline{z_0}(z_0 - z^*)^2}\right] - \frac{X_0'(z_0)}{1-g}\left[\frac{h\gamma_2 R}{z_0}\exp\left[\frac{\mathrm{i}}{2}(\alpha_1+\alpha_2) + \beta(\alpha_2 - \alpha_1 - 2\pi)\right]\right. \\ & + D_0 K z_0 + h\gamma_2 - R\left(\frac{1}{2}\exp[\mathrm{i}\alpha_1] + \frac{1}{2}\exp[\mathrm{i}\alpha_2] + \mathrm{i}\beta\exp[\mathrm{i}\alpha_1] - \mathrm{i}\beta\exp[\mathrm{i}\alpha_2]\right)KD_0 \\ & + \frac{h\overline{\gamma_2}}{X_0(z^*)}\frac{z^*}{\overline{z_0}(z_0 - z^*)} - \frac{h\overline{\gamma_2}}{X_0(z^*)}\frac{z^*}{\overline{z_0}}\frac{X_0'(z^*)}{X_0(z^*)} - \frac{h\gamma_2}{X_0(z^*)}\frac{1}{z_0 - z^*}\Big] - \frac{X_0(z_0)}{1-g}\left[-\frac{h\gamma_2 R}{z_0^2}\exp\left[\frac{\mathrm{i}}{2}(\alpha_1+\alpha_2)\right.\right. \\ & \left. + \beta(\alpha_2 - \alpha_1 - 2\pi)\right] + KD_0 - \frac{2h\overline{\gamma_2}}{X_0(z^*)}\frac{z^*}{\overline{z_0}(z_0 - z^*)^2} + \frac{h\overline{\gamma_2}}{X_0(z^*)}\frac{X_0'(z^*)}{X_0(z^*)}\frac{z^*}{\overline{z_0}(z_0 - z^*)} \\ & \left. + \frac{h\gamma_2}{X_0(z^*)}\frac{1}{(z_0 - z^*)^2}\right] - \frac{h\gamma_2}{1-g}\frac{X_0''(z_0)}{2X_0(z_0)}\end{aligned} \tag{51}$$

$$\begin{aligned}\Psi_2^*(z_0) = {} & \frac{R^2}{z_0^2}\left[\Phi_2^*(z_0) - z_0\Phi_z^{*\prime}(z_0)\right] + \frac{R^2}{z_0^2}\left\{\frac{K}{1-g}\left(\frac{\overline{\gamma_2} z_0}{R^2 - z_0\overline{z_0}} + \frac{\overline{\gamma_2} z_0}{R^2} + \overline{D_0}\right)\right. \\ & - \frac{\overline{X}_0(R^2/z_0)}{1-g}\left[\frac{h\overline{\gamma_2} z_0}{R}\exp\left[\frac{-\mathrm{i}}{2}(\alpha_1+\alpha_2) + \beta(\alpha_2 - \alpha_1 - 2\pi)\right] + \frac{R^2}{z_0}K\overline{D_0} + h\overline{\gamma_2}\right. \\ & \left. - R\left(\frac{1}{2}\exp[-\mathrm{i}\alpha_1] + \frac{1}{2}\exp[-\mathrm{i}\alpha_2] - \mathrm{i}\beta\exp[-\mathrm{i}\alpha_1] + \mathrm{i}\beta\exp[-\mathrm{i}\alpha_2]\right)K\overline{D_0} + \frac{h\overline{\gamma_2}}{\overline{X_0(z_0)}}\frac{z_0}{R^2 - z_0\overline{z_0}}\right] \\ & \left. + \frac{h\overline{\gamma_2}}{1-g}\frac{\overline{X}_0'(R^2/z_0)}{\overline{X}_0(R^2/z_0)} + \frac{\gamma_2(z_0\overline{z_0} - R^2)}{R^2 z_0} + \frac{\overline{\gamma_2} z_0}{R^2}\right\} - \frac{2\overline{\gamma_2}}{z_0} - \frac{\gamma_2\overline{z}_0}{z_0^2}\end{aligned} \tag{52}$$

Substituting Eqs. (50)–(52) into Eq. (42), a closed form expression of the force on the dislocation can be obtained.

If $\alpha_1 = \alpha_2 = 0$, and the edge dislocation with the Burger's vector $(b_x, 0)$ is located at any point x_0 $(x_0 > R)$ on the x-axis, the force on the dislocation is reduce to

$$\begin{aligned}F_x = {} & \frac{-\mu_2 b_x^2}{\pi(1+\kappa_2)}\left\{\left(1 - \frac{h}{g}\right)\left[\frac{-1}{x_0} + \left(x_0^3 + 2R^2 x_0 + \frac{R^6 - 4R^4 x_0^2}{x_0^3}\right)\frac{1}{(x_0^2 - R^2)^2} + \frac{2R^2}{x_0(R^2 - x_0^2)} + \frac{2R^2}{x_0^2}\right]\right. \\ & \left. + (1+h)\frac{R^4}{x_0^3(R^2 - x_0^2)}\right\}\end{aligned} \tag{53}$$

$$F_y = 0 \tag{54}$$

which are in agreement with the results of Dundurs and Mura (1964).

4.2. Edge dislocation inside the inhomogeneity

Similarly, when the edge dislocation is located at the point z_0 in the inhomogeneity, the perturbation stresses can be evaluated by the perturbation stress functions $\Phi_1^*(z_0)$, $\Phi_1^{*\prime}(z_0)$ and $\Psi_1^*(z_0)$ in the inhomogeneity. In terms of Eq. (41) the Peach–Keohler force can be expressed as

$$F_x - \mathrm{i}F_y = \frac{\mu_1(b_y^2 + b_x^2)}{\pi(1+\kappa_1)}\left[\frac{\Phi_1^*(z_0) + \overline{\Phi_1^*(z_0)}}{\gamma_1} + \frac{\overline{z}_0\Phi_1^{*\prime}(z_0) + \Psi_1^*(z_0)}{\overline{\gamma_1}}\right] \tag{55}$$

where

$$\begin{aligned}\Phi_1^*(z_0) = &-\frac{h}{1-g}\left[\frac{\gamma_2}{z_0} - \frac{\gamma_1}{z_0 - z^*} + \frac{\overline{\gamma_1}z^*}{\overline{z_0}(z_0 - z^*)} + D_0^*\right] + \frac{X_0(z_0)}{1-g}\left[\frac{h\gamma_2 R}{z_0}\exp\left[\frac{\mathrm{i}}{2}(\alpha_1+\alpha_2) + \beta(\alpha_2 - \alpha_1 - 2\pi)\right]\right.\\ &+ KD_0^* z_0 + h\gamma_2 - R\left(\frac{1}{2}\exp[\mathrm{i}\alpha_1] + \frac{1}{2}\exp[\mathrm{i}\alpha_2] + \mathrm{i}\beta\exp[\mathrm{i}\alpha_1] - \mathrm{i}\beta\exp[\mathrm{i}\alpha_2]\right)KD_0^*\\ &\left.+ \frac{K\overline{\gamma_1}}{X_0(z^*)}\frac{z^*}{\overline{z_0}(z_0 - z^*)} - \frac{K\overline{\gamma_1}}{X_0(z^*)}\frac{z^*}{\overline{z_0}}\frac{X_0'(z^*)}{X_0(z^*)} - \frac{K\gamma_1}{X_0(z^*)}\frac{1}{z_0 - z^*}\right] + \frac{K\gamma_1}{1-g}\frac{X_0'(z_0)}{X_0(z_0)}\end{aligned} \tag{56}$$

$$\begin{aligned}\Phi_1^{*\prime}(z_0) = &-\frac{h}{1-g}\left[-\frac{\gamma_2}{z_0^2} + \frac{\gamma_1}{(z_0 - z^*)^2} - \frac{2\overline{\gamma_1}z^*}{\overline{z_0}(z_0 - z^*)^2}\right] + \frac{X_0'(z_0)}{1-g}\left[\frac{h\gamma_2 R}{z_0}\exp\left[\frac{\mathrm{i}}{2}(\alpha_1+\alpha_2) + \beta(\alpha_2 - \alpha_1 - 2\pi)\right]\right.\\ &+ KD_0^* z_0 + h\gamma_2 - R\left(\frac{1}{2}\exp[\mathrm{i}\alpha_1] + \frac{1}{2}\exp[\mathrm{i}\alpha_2] + \mathrm{i}\beta\exp[\mathrm{i}\alpha_1] - \mathrm{i}\beta\exp[\mathrm{i}\alpha_2]\right)KD_0^*\\ &+ \frac{K\overline{\gamma_1}}{X_0(z^*)}\frac{z^*}{\overline{z_0}(z_0 - z^*)} - \frac{K\overline{\gamma_1}}{X_0(z^*)}\frac{z^*}{\overline{z_0}}\frac{X_0'(z^*)}{X_0(z^*)} - \frac{K\gamma_1}{X_0(z^*)}\frac{1}{z_0 - z^*}\Big] + \frac{X_0(z_0)}{1-g}\left[-\frac{h\gamma_2 R}{z_0^2}\exp\left[\frac{\mathrm{i}}{2}(\alpha_1+\alpha_2)\right.\right.\\ &\left.\left.+ \beta(\alpha_2 - \alpha_1 - 2\pi)\right] + KD_0^* - \frac{2K\overline{\gamma_1}}{X_0(z^*)}\frac{z^*}{\overline{z_0}(z_0 - z^*)^2} + \frac{K\overline{\gamma_1}}{X_0(z^*)}\frac{X_0'(z^*)}{X_0(z^*)}\frac{z^*}{\overline{z_0}(z - z^*)} + \frac{K\gamma_1}{X_0(z^*)}\frac{1}{(z_0 - z^*)^2}\right]\\ &+ \frac{K\gamma_1}{1-g}\frac{X_0''(z_0)}{2X_0(z_0)}\end{aligned} \tag{57}$$

$$\begin{aligned}\Psi_1^*(z_0) = &\frac{R^2}{z_0^2}\left[\Phi_1^*(z_0) - z_0\Phi_1^{*\prime}(z_0)\right]\frac{R^2}{z_0^2}\left\{\frac{-h}{1-g}\left(\frac{\overline{\gamma_1}z_0}{R^2 - z_0\overline{z_0}} + \overline{D_0^*} + \frac{\overline{\gamma_2}z_0}{R^2}\right)\right.\\ &+ \frac{\overline{X}_0(R^2/z_0)}{1-g}\left[\frac{h\overline{\gamma_2}z_0}{R}\exp\left[\frac{-\mathrm{i}}{2}(\alpha_1+\alpha_2) + \beta(\alpha_2 - \alpha_1 - 2\pi)\right] + \frac{R^2}{z_0}K\overline{D_0^*} + h\overline{\gamma_2}\right.\\ &\left.- R\left(\frac{1}{2}\exp[-\mathrm{i}\alpha_1] + \frac{1}{2}\exp[-\mathrm{i}\alpha_2] - \mathrm{i}\beta\exp[-\mathrm{i}\alpha_1] + \mathrm{i}\beta\exp[-\mathrm{i}\alpha_2]\right)K\overline{D_0^*} + \frac{hK\overline{\gamma_1}}{\overline{X_0(z_0)}}\frac{z_0}{R^2 - z_0\overline{z_0}}\right]\\ &\left.+ \frac{K\overline{\gamma_1}}{1-g}\frac{\overline{X}_0'(R^2/z_0)}{\overline{X}_0(R^2/z_0)} + \frac{\gamma_1(z_0\overline{z_0} - R^2)}{R^2 z_0} + \frac{\overline{\gamma_1}z_0}{R^2}\right\} - \frac{2\overline{\gamma_1}}{z_0} - \frac{\gamma_1\overline{z}_0}{z_0^2}\end{aligned} \tag{58}$$

If $\alpha_1 = \alpha_2 = 0$, and the edge dislocation with the Burger's vector $(b_x, 0)$ is located at a point x_0 $(x_0 < R)$ on the x-axis, the force on the dislocation can be reduced to Eq. (15) in the paper of Dundurs and Sendeckyj (1965).

4.3. Straight crack along the interface of two dissimilar materials

Consider the problem of a straight crack from l_1 to l_2 on the y-axis which lies along the interface between two dissimilar materials, as shown in Fig. 2. An edge dislocation with Burger's vector (b_x, b_y) acts at an arbitrary point in the medium II. In this case, the solution can be easily derived from our general formulations by letting the radius R of the circular inhomogeneity tend to infinity and the angles α_1 and α_2 approach to zero such that $R\alpha_1 = l_1$ and $R\alpha_2 = l_2$. Accordingly, the force on the dislocation can be obtained from Eqs. (50)–(52).

$$\Phi_2^*(z_0) = \frac{K}{1-g}\frac{\overline{\gamma_2}-\gamma_2}{z_0-\overline{z_0}} - \frac{X_0(z_0)}{1-g}\left[-\frac{h\gamma_2}{g} + h\gamma_2 + \frac{h\overline{\gamma_2}}{X_0(\overline{z_0})}\frac{1}{(z_0-\overline{z_0})} - \frac{h\overline{\gamma_2}}{X_0(\overline{z_0})}\frac{X_0'(\overline{z_0})}{X_0(\overline{z_0})} - \frac{h\gamma_2}{X_0(\overline{z_0})}\frac{1}{z_0-\overline{z_0}}\right] - \frac{h\gamma_2}{1-g}\frac{X_0'(z_0)}{X_0(z_0)} \tag{59}$$

$$\begin{aligned}\Phi_2^{*\prime}(z_0) = {} & \frac{K}{1-g}\left[\frac{\gamma_2}{(z_0-\overline{z_0})^2} - \frac{2\overline{\gamma_2}}{(z_0-\overline{z_0})^2}\right] - \frac{X_0'(z_0)}{1-g}\left[-\frac{h\gamma_2}{g} + h\gamma_2 + \frac{h\overline{\gamma_2}}{X_0(\overline{z_0})}\frac{1}{(z_0-\overline{z_0})} - \frac{h\overline{\gamma_2}}{X_0(\overline{z_0})}\frac{X_0'(\overline{z_0})}{X_0(\overline{z_0})}\right. \\ & \left. - \frac{h\gamma_2}{X_0(\overline{z_0})}\frac{1}{z_0-\overline{z_0}}\right] - \frac{X_0(z_0)}{1-g}\left[\frac{h\gamma_2}{gz_0} - \frac{2h\overline{\gamma_2}}{X_0(\overline{z_0})}\frac{1}{(z_0-\overline{z_0})^2} + \frac{h\overline{\gamma_2}}{X_0(\overline{z_0})}\frac{X_0'(\overline{z_0})}{X_0(\overline{z_0})}\frac{1}{(z_0-\overline{z_0})}\right. \\ & \left. + \frac{h\gamma_2}{X_0(\overline{z_0})}\frac{1}{(z_0-\overline{z_0})^2}\right] - \frac{h\gamma_2}{1-g}\frac{X_0''(z_0)}{2X_0(z_0)}\end{aligned} \tag{60}$$

$$\begin{aligned}\Psi_2^*(z_0) = {} & \frac{-2\overline{\gamma_2}}{z_0} - \frac{\gamma_2\overline{z}_0}{z_0^2} + \Phi_2^*(z_0) - z_0\Phi_2^{*\prime}(z_0) + \frac{K}{1-g}\left(\frac{\overline{\gamma_2}z_0}{\overline{z_0^2 - z_0\overline{z_0}}} + \frac{\overline{\gamma_2}}{z_0}\right) \\ & - \frac{X_0(z_0)}{1-g}\left[-\frac{h\overline{\gamma_2}}{g} + h\overline{\gamma_2} + \frac{h\overline{\gamma_2}}{\overline{X_0(z_0)}}\frac{z_0}{\overline{z_0}-z_0}\right] + \frac{h\overline{\gamma_2}}{1-g}\frac{X_0'(z_0)}{X_0(z_0)} + \frac{\gamma_2(z_0-\overline{z_0})}{z_0\overline{z_0}} + \frac{\overline{\gamma_0}}{z_0}\end{aligned} \tag{61}$$

where $X_0(z_0) = (z_0 - l_1)^{\frac{-1}{2}-i\beta}(z_0 - l_2)^{\frac{-1}{2}+i\beta}$

Substituting Eqs. (59)–(61) into Eq. (42), we obtain the image force on the dislocation due to an interaction with a straight interfacial crack. As far as we can see it is a new solution.

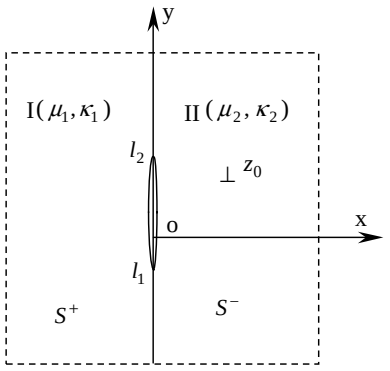

Fig. 2. An edge dislocation interacting with a straight interfacial crack.

5. Numerical analysis and discussion

For the convenience of comparing with the previous known solutions, we consider the special case that an arc-crack is symmetrically placed with respect to the x-axis ($\alpha_2 = -\alpha_1 = \alpha$) and an edge dislocation lies on the x-axis ($z_0 = x_0 > R$ is a real number) as shown in Fig. 3. Using Eq. (42), the influence of the circular interfacial crack upon the image force is discussed in this section. We define the normalized force on the dislocation as

$$F_{x0} = \pi R(1+\kappa_2)F_1/\mu_2 b_x^2 \quad F_{y0} = \pi R(1+\kappa_2)F_2/\mu_2 b_y^2 \tag{62}$$

where F_1 is the force on the gliding dislocation b_x (Burger's vector $(b_x, 0)$), and F_2 is the force on the climbing dislocation b_y (Burger's vector $(0, b_y)$).

In the general plane strain case ($\kappa = 3 - 4\nu$), the influence of the crack geometry and material properties on the image force F_1 is shown in Figs. 4–6. First, we let $\kappa_1 = \kappa_2 = 1.8$. The normalized force F_{x0} on the dislocation versus $\lambda = x_0/R$ for different values of $m = \mu_1/\mu_2$ is depicted in Fig. 4(a) ($\alpha = 0$) and Fig. 4(b) ($\alpha = 0.1$). It is seen that F_{x0} is always positive (repels the dislocation in the matrix) for $m > 1$ and always negative (attracts the dislocation in the matrix) for $m < 1$ as $\alpha = 0$. If $\alpha = 0.1$ (a crack is present), F_{x0} is always negative for $m \leqslant 1$ and the crack attracts the dislocation. F_{x0} is positive first, then becomes negative when the edge dislocation approaches to the interface from infinity along the x-axis for $m > 1$. There is an equilibrium position on the x-axis and the image force is equal to zero at that point. The image force also achieves a positive maximum value (repulsion force) on the x-axis. For all values of m ($m \leqslant 1$ and $m > 1$), the magnitude of the attraction force on the dislocation will be a large value when the dislocation approaches to the interfacial crack. Comparison between Fig. 4(a) and (b) shows that the interfacial crack attracts the edge dislocation in the matrix.

Let $\kappa_1 = 1.8$ and $m = 1$. The normalized force F_{x0} on the dislocation versus $\lambda = x_0/R$ for different κ_2 is plotted in Fig. 5(a) ($\alpha = 0$) and in Fig. 5(b) ($\alpha = 0.1$). It is seen that F_{x0} is always positive (repels the dislocation in the matrix) as $\kappa_2 > \kappa_1$ and always negative (attracts the dislocation in the matrix) as $\kappa_2 < \kappa_1$ in the case of $\alpha = 0$. If $\alpha = 0.1$ (a crack is present), the force on the dislocation is always negative, which differs from the variations of the curve in Fig. 4(b). From Figs. 4 and 5, we see that as $\lambda = z_0/R > 2$, the material elastic constants and crack dimension have little effect on the dislocation force.

The variation of the normalized force F_{x0} acting on the dislocation with the crack radius α is plotted in Fig. 6 for different values of m ($\lambda = 1.1$ and $\kappa_1 = \kappa_2 = 1.8$). It is seen that when $m > 1$, the interfacial crack has significant influence upon the force on the dislocation and there exists a critical value of the crack radius

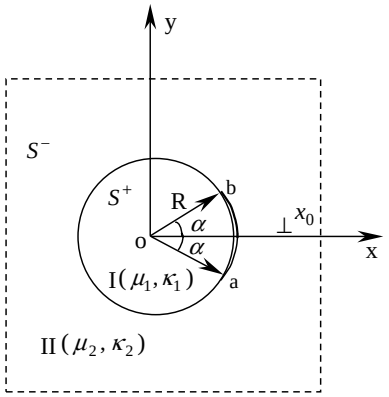

Fig. 3. An edge dislocation interacting with an interfacial crack symmetrically with respect to the axis.

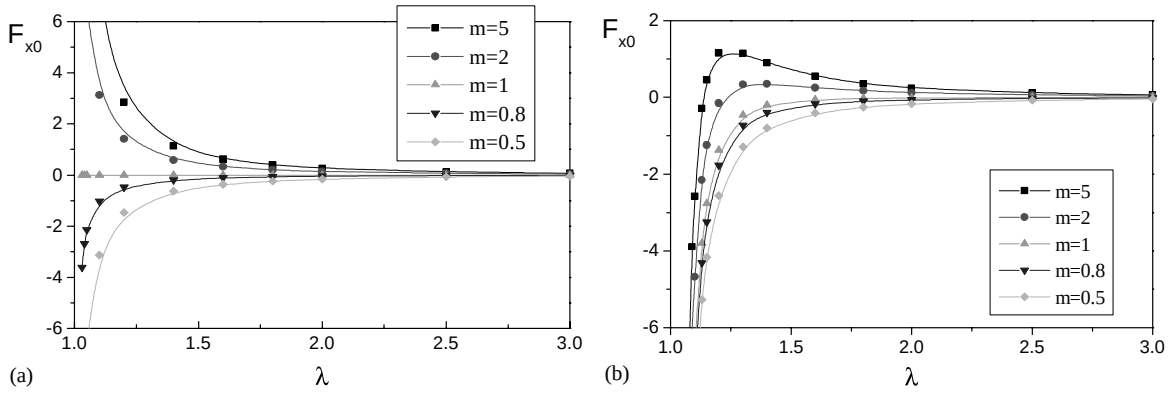

Fig. 4. Normalized force F_{x0} versus $\lambda = x_0/R$ for various values of m as (a) $\alpha = 0$ and $\kappa_1 = \kappa_2 = 1.8$ and (b) $\alpha = 0.1$ and $\kappa_1 = \kappa_2 = 1.8$.

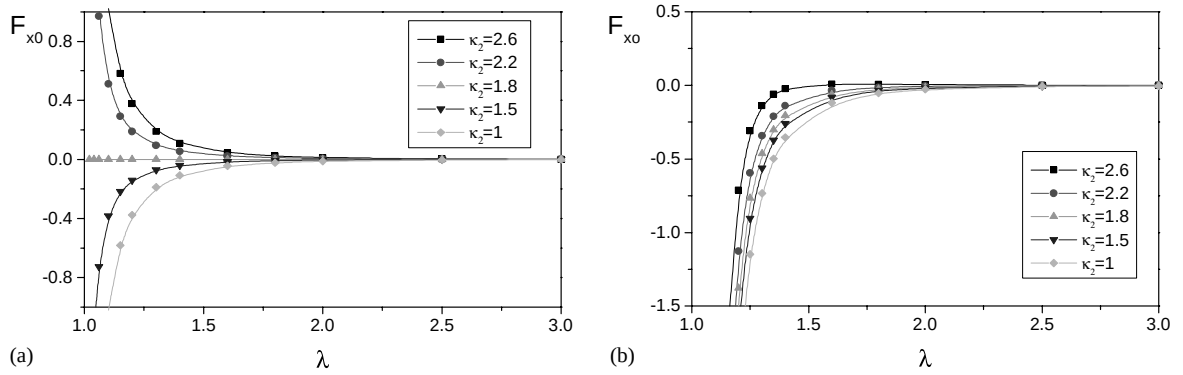

Fig. 5. Normalized force F_{x0} versus $\lambda = x_0/R$ for various values of κ_2 as (a) $\alpha = 0$ and $\kappa_1 = 1.8$, $m = 1$ and (b) $\alpha = 0.1$ and $\kappa_1 = 1.8$, $m = 1$.

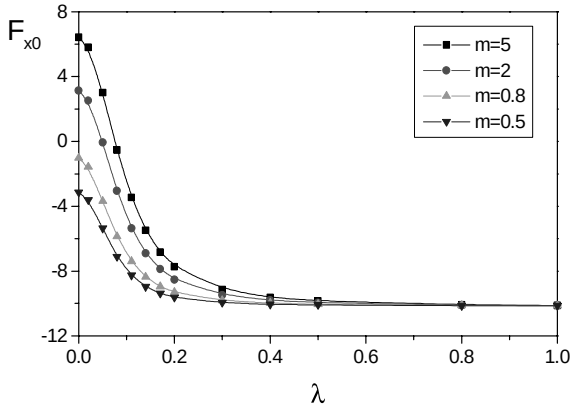

Fig. 6. Normalized force F_{x0} versus α for various values of m as $\lambda = z_0/R = 1.1$ and $\kappa_1 = \kappa_2 = 1.8$.

altering the direction of the image force. The attraction force on the dislocation will increase with the increment of the crack radius.

The influence of the crack dimensions and elastic material constants on the image force F_2 is shown in Figs. 7–9. Let $\kappa_1 = \kappa_2 = 1.8$. The normalized force F_{y0} on the dislocation versus $\lambda = x_0/R$ for different

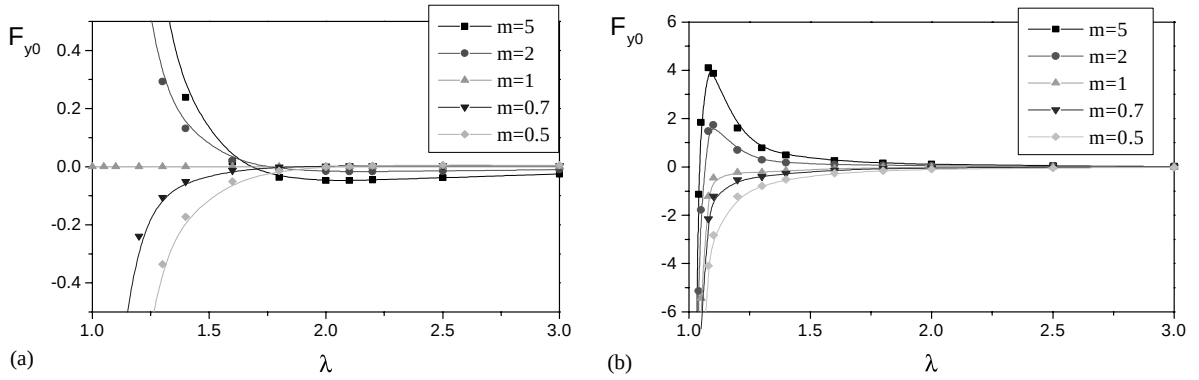

Fig. 7. Normalized force F_{y0} versus $\lambda = x_0/R$ for various values of m as (a) $\alpha = 0.1$ and $\kappa_1 = \kappa_2 = 1.8$ and (b) $\alpha = 0.2$ and $\kappa_1 = \kappa_2 = 1.8$.

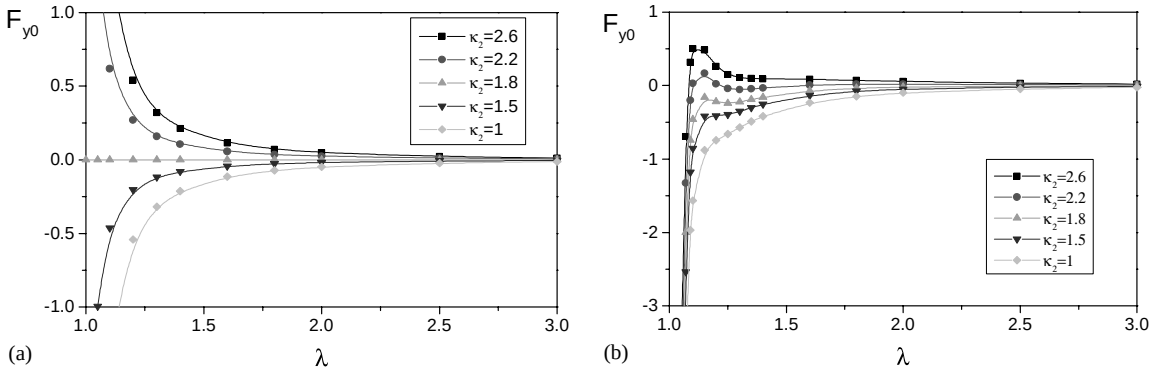

Fig. 8. Normalized force F_{y0} versus $\lambda = x_0/R$ for various values of κ_2 as (a) $\alpha = 0$ and $\kappa_1 = 1.8$, $m = 1$ and (b) $\alpha = 0.2$ and $\kappa_1 = 1.8$, $m = 1$.

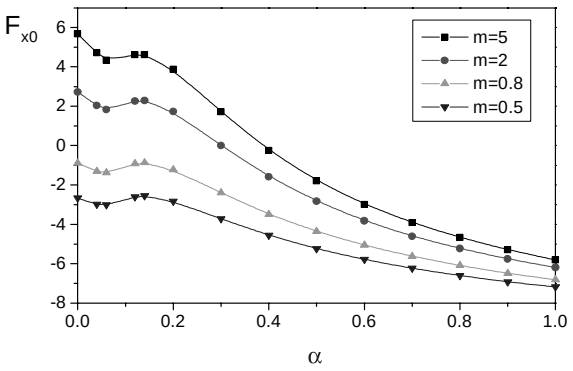

Fig. 9. Normalized force F_{y0} versus α for various values of m as $\lambda = z_0/R = 1.1$ and $\kappa_1 = \kappa_2 = 1.8$.

values of $m = \mu_1/\mu_2$ is depicted in Fig. 7(a) ($\alpha = 0$) and in Fig. 7(b) ($\alpha = 0.2$). It is found that, differing from F_{x0}, for all values of m ($m \leqslant 1$ and $m > 1$), F_{y0} always has an equilibrium point on the x-axis when the edge dislocation approaches to the interface from infinity in the case $\alpha = 0$. As $\alpha = 0.2$, the variations shown in Fig. 7(b) are in the similitude of F_{x0}. However, the variation of F_{y0} is more acute than those of F_{x0} when the distance between the edge dislocation and the interface is very small. Similarly, the attraction force on a dislocation will become very large when the dislocation approaches to the interfacial crack for all values of m ($m \leqslant 1$ and $m > 1$).

Let $\kappa_1 = 1.8$ and $m = 1$. The normalized force F_{y0} on the dislocation versus $\lambda = x_0/R$ for different values of κ_2 is plotted in Fig. 8(a) ($\alpha = 0$) and in Fig. 8(b) ($\alpha = 0.2$). Similarly, F_{y0} is always positive (repels dislocation in the matrix) for $\kappa_2 > \kappa_1$ and always negative (attracts the dislocation in the matrix) for $\kappa_2 < \kappa_1$ as $\alpha = 0$. As $\alpha = 0.2$ and $\kappa_2 > \kappa_1$, the variations of F_{y0} differs from those of F_{x0} shown in Fig. 5(b). There is an equilibrium position on the x-axis whereF_{y0} is equal to zero. In addition, following the discussion in the above paragraph, results similar to those in Fig. 8 can be obtained.

The variation of the normalized force F_{y0} acting on a dislocation with the crack radius α is plotted in Fig. 9 for different values of m ($\lambda = 1.1$ and $\kappa_1 = \kappa_2 = 1.8$). It is shown that when $m > 1$, the interfacial crack has significant influence upon the force on a dislocation and there exists a critical value of the crack radius altering the direction of the image force. The attraction force on a dislocation will increase with the increase of the crack radius; however it will decrease as the crack radius α varies from 0.06 to 0.14.

6. Conclusions

Using Muskhelishvili's complex variable method, the closed form complex potentials are obtained for an edge dislocation, which is located either inside the matrix or inhomogeneity, interacting with an interfacial crack in this paper. Analytical expressions of the image force on the dislocation are also given. In Section 5, the influence of the crack geometry and material mismatch on the dislocation force is discussed graphically. The results indicate that the interfacial crack plays an important role in the Peach–Keohler dislocation force. When the length of a crack goes up to some critical value, the presence of the interfacial crack can change the interaction mechanism between an edge dislocation and a circular inhomogeneity. The closed form solutions of Eqs. (28), (29) and (38), (39) can be used as Green's functions to solve the problem of interaction between an interfacial crack and an arbitrary shape crack inside the matrix or inhomogeneity.

Acknowledgements

The authors would like to thank the support by the National Natural Science Foundation of China under grant NNSFC 10272009 and the Natural Science Foundation of Hunan Province.

References

Dundurs, J., 1969. Mathematical Theory of Dislocations. In: Mura, T. ASME, pp. 70–115.

Dundurs, J., Mura, T., 1964. Interaction between an edge dislocation and a circular inclusion. Journal of Mechanics and Physics of Solids 12, 177–189.

Dundurs, J., Sendeckyj, G.P., 1965. Edge dislocation inside a circular inclusion. Journal of Mechanics and Physics of Solids 13, 141–147.

Gong, S.X., Meguid, S.A., 1994. A screw dislocation interaction with an elastic elliptical inhomogeneity. International Journal of Engineering Science 32, 1221–1228.

Head, A.K., 1953. The interaction of dislocations boundaries. Philosophical Magazine 44, 92–94.

Hirth, J.P., Lothe, J., 1982. Theory of Dislocations, second ed. John Wiley, New York.
Lee, S.B., 1987. The image force on the screw dislocation around crack of finite size. Engineering Fracture Mechanics 27, 539–545.
Liu, Y.W., 1991. Base singular solutions of antiplane problem on circular-arc cracks between bonded dissimilar materials. ACTA Mechanics Solida Sinica 12, 244–254.
Lung, C.W., Wang, L., 1984. Image force on the dislocation near a finite length crack tip. Philosophical Magazine A 50 (5), L19–L22.
Luo, H.A., Chen, Y., 1991. An edge dislocation in a three-phase composites cylinder. ASME Journal of Applied Mechanics 58, 75–86.
Muskhelishvili, N.L., 1975. Some Basic problems of Mathematical Theory of Elasticity. Noordhoff, Leyden.
Qaissaunee, M.T., Santare, M.H., 1995. Edge dislocation interaction with an elliptical inclusion surrounding by an interfacial zone. Quarter Journal Mechanics and Applied Mathematic 48, 465–482.
Smith, E., 1968. The interaction between dislocation and inhomogeneities-1. International Journal of Engineering Science 6, 129–143.
Toya, M., 1974. A crack along the interface of a circular inclusion embedded in an infinite solid. Journal of Mechanics and Physics of Solids 22, 325–348.
Xiao, Z.A., Chen, B.J., 2000. A screw dislocation interacting with a coated fiber. Mechanics of Materials 32, 485–494.
Xiao, Z.A., Chen, B.J., 2001. On interaction between an edge dislocation and a coated inclusion. International Journal Solids and Structure 38, 2533–2548.